Journal of Molecular Structure 977 (2010) 117–129

Contents lists available at ScienceDirect

Journal of Molecular Structure

journal homepage: www.elsevier.com/locate/molstruc

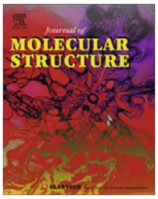

Crystal structures and vibrational spectra of novel compounds with dimeric glycine glycinium cations

V.V. Ghazaryan [a], M. Fleck [b], A.M. Petrosyan [a,*]

[a] *Institute of Applied Problems of Physics, NAS of Armenia, 25 Nersessyan Str., 0014 Yerevan, Armenia*
[b] *Institute of Mineralogy and Crystallography, University of Vienna, Althanstr. 14, A-1090 Vienna, Austria*

ARTICLE INFO

Article history:
Received 6 March 2010
Received in revised form 13 May 2010
Accepted 13 May 2010
Available online 20 May 2010

Keywords:
Glycine glycinium salts
Crystal structure
Vibrational spectra

ABSTRACT

The glycinium compounds glycine glycinium tetrafluoroborate ($GlyH\cdot Gly\cdot BF_4$) (I), glycine glycinium perchlorate ($GlyH\cdot Gly\cdot ClO_4$) (II), glycinium tetrafluoroborate ($GlyH\cdot BF_4$) (III), glycinium perchlorate ($GlyH\cdot ClO_4$) (IV), and glycine glycinium iodide ($GlyH\cdot Gly\cdot I$) (V) have been synthesized, (I–IV) for the first time. The crystal structures could be determined for (I), (II), and (V), the first two represent novel species and have therefore been characterized by vibrational spectroscopy as well. Compounds (III) and (IV) proved unstable and are characterized by vibrational spectroscopy only. The results of the redetermination of (V) are compared with previously reported data. The crystal structures comprise dimeric cations of the type ($GlyH\cdots Gly$) connected to monovalent anions via hydrogen bonds.

1. Introduction

Among salts of amino acids that are recently being studied intensively, there is a class of salts with the composition $2A\cdot HX$, in which the cation is a dimer of the type $(AH\cdots A)^+$, where A is amino acid in its zwitterionic state and AH is protonated at the expense of the acid HX, i.e. the composition can more accurately be given as $(AH\cdots A)^+\cdot X^-$. The molecules A and AH are connected to each other via a characteristically short hydrogen bond. This class of compounds represents an interesting issue from different points of view, i.e. as species with short hydrogen bonds, crystals in which phase transitions are possible, and additionally, many of them as nonlinear optical materials.

The systematic study of $2A\cdot HX$ type salts was started by Frost, who prepared diglycine chloride, diglycine bromide, diglycine iodide and tried to prepare diglycine fluoride and similar compounds of dialanine [1]. One of these, namely diglycine chloride, as well as diglycine nitrate, were known since the 19th century (see Refs. in [1]). Subsequently, the crystal structures of the first two crystals grown by Frost have been determined [2,3] and thus the existence of dimeric cations was established. Eventually, the structure of the third crystal was also determined [4], and it turned out that it is formed by the same mechanism, comprising $(Gly\cdots Gly^+)\cdot I^-$. Interest in crystalline salts of glycine (and other amino acids) with dimeric cations increased even more after the observation of a ferroelectric phase transition in diglycine nitrate [5], which later became a subject of numerous works. In addition to the above mentioned crystals, dimeric cations were observed in the structures of the following salts of glycine: diglycine picrate [6], diglycine hydrogen selenite [7], monoclinic and triclinic forms of diglycine perrhenate [8,9] and diglycine fumarate monohydrate [10]. An overview of the glycine glycinium compounds presently known is given in Table 1.

In addition, we report the synthesis and characterization of two novel salts of this type, viz. diglycine tetrafluoroborate and diglycine perchlorate. In the systems glycine—HBF_4—H_2O and glycine—$HClO_4$—H_2O, the formation of compounds with a 1:1 ratio has also been observed. However, glycinium tetrafluoroborate and glycinium perchlorate are less stable than the corresponding 2:1 compounds, due to their hygroscopicity. We have, therefore, focused our attention on glycine glycinium tetrafluoroborate, ($GlyH\cdot Gly\cdot BF_4$) (I), and glycine glycinium perchlorate, ($GlyH\cdot Gly\cdot ClO_4$) (II), in the present work. The 1:1 compounds, glycinium tetrafluoroborate ($GlyH\cdot BF_4$) (III), glycinium perchlorate ($GlyH\cdot ClO_4$) (IV), are characterized only by their vibrational spectra. The structure of glycine glycinium iodide ($GlyH\cdot Gly\cdot I$) (V) was redetermined and compared with the previously reported data.

The crystal structures of diglycine chloride, diglycine bromide, and diglycine nitrate, which were originally determined by photographic methods, were later reinvestigated [11–15]. Strangely enough, the structure of glycine glycinium iodide ($GlyH\cdot Gly\cdot I$) (V) was not reinvestigated since [4]. Hence we conducted a reinvestigation of this species and include the results in this work. Although the general features of the original structure were confirmed, some details differ significantly.

---

* Corresponding author. Tel.: +374 10 241106; fax: +374 10 281861.
E-mail address: apetros@iapp.sci.am (A.M. Petrosyan).

0022-2860/$ - see front matter © 2010 Elsevier B.V. All rights reserved.
doi:10.1016/j.molstruc.2010.05.022

Table 1
Unit cell parameters, space group and Z of crystallographically characterized glycine glycinium compounds.

Compound	a (Å)	b (Å)	c (Å)	α (°)	β (°)	γ (°)	s.g., Z	Refs.
2Gly·HCl	5.2992(6)	8.083(2)	17.973(2)	90	90	90	$P2_12_12_1$, 4	[11]
2Gly·HBr	5.385(1)	8.199(2)	18.402(3)	90	90	90	$P2_12_12_1$, 4	[13]
2Gly·HI	18.589(4)	5.161(1)	20.389(4)	90	110.67(3)	90	$C2$, 8	[a]
2Gly·HNO_3	9.460(1)	5.1728(5)	9.224(1)	90	97.217(15)	90	$P2_1/a$, 2	[14]
2Gly·H_2SeO_3	12.2651(7)	4.8079(6)	19.955(1)	90	122.745(4)	90	$P2_1/c$, 4	[7]
2Gly·$HReO_4$	15.7095(5)	8.1826(3)	8.2909(3)	90	103.715(2)	90	$P2_1/c$, 4	[8]
2Gly·$HReO_4$	5.2688(2)	9.4982(3)	10.5374(3)	79.458(2)	78.811(2)	76.383(2)	$P1$, 2	[9]
2Gly·HBF_4	8.6069(2)	11.8626(3)	14.7597(4)	104.451(1)	106.417(1)	94.918(1)	$P\bar{1}$, 6	[a]
2Gly·$HClO_4$	8.700(2)	14.842(2)	19.396(2)	98.748(7)	93.056(9)	106.053(9)	$P\bar{1}$, 10	[a]
2Gly picrate	14.968(3)	6.722(2)	15.165(3)	90	93.65(2)	90	$P2_1/a$, 4	[6]
2Gly fumarate·H_2O	13.058(1)	6.8251(7)	15.326(1)	90	112.65(2)	90	$P2_1/n$, 4	[10]

[a] This work.

2. Experimental section

2.1. Materials and synthesis

All the reagents were purchased from commercial sources and used as received. Crystals of compound 2Gly·HI (V) were obtained following the description in Ref. [1]. Originally the compounds 2Gly·HBF_4 (I) and 2Gly·$HClO_4$ (II) were obtained as by-products from the aqueous solutions containing glycine, HF, HBF_4 in molar ratio 2:1:1 and glycine, HF, $HClO_4$ in the same 2:1:1 M ratio during our on-going study on searching of new mixed salts of amino acids. Then we studied the systems Gly + HF + H_2O and Gly + HBF_4 ($HClO_4$) + H_2O in more detail. We found that (I) and (II) can be prepared from aqueous solutions containing stoichiometric quantities of respective components by usual slow evaporation technique. From the solutions containing equimolar quantities of components the compounds Gly·HBF_4 (III) and Gly·$HClO_4$ (IV) can be obtained, which turned to be very hygroscopic. Probably this was the reason why the crystals (I) and (II) escaped researchers' attention to date.

2.2. Crystal structure determination

Single-crystal X-ray intensity data of the compounds 2Gly·HBF_4 (I), 2Gly·$HClO_4$ (II), and 2Gly·HI (V) were collected on the following diffractometer types, all of which employed graphite-monochromated Mo Kα radiation (λ = 0.71073 Å) and CCD area detectors: Bruker-APEX II (compounds I and II), and Bruker–Nonius Kappa (compound V). The intensity data were processed with the Bruker–Nonius program suites Collect [16] and Saint-Plus [17] and corrected for Lorentz, polarization, background and absorption effects [17,18]. The crystal structures were determined by direct methods and subsequent Fourier and difference Fourier syntheses, followed by full-matrix least-squares refinements on F^2 [19]. Scattering factors for neutral atoms were employed in the refinements.

In the refinement processes of I and II, hydrogen atoms were placed at geometrically calculated positions, then treated as riding on their parent atom, with free refinement of the isotropic displacement parameters (except for one atom, H1c, in II). For compound V, all hydrogen atoms were located from the difference Fourier maps and refined freely. All non-H atoms were refined anisotropically and all hydrogen atoms isotropically. In compound I, the fluorine atoms of the BF_4-group show large displacement parameters, which is usual in likewise chemical environments. The final $R1$-values of the refinements were 0.056, 0.057, and 0.032, respectively, for I, II, and V. Crystal data, details of the measurement and refinement are given in Table 2. Supplementary crystallographic data for this paper have been deposited. These data can be obtained free of charge via www.ccdc.cam.ac.uk/conts/retrieving.html (or from the Cambridge Crystallographic Data Centre, 12 Union Road, Cambridge CB2 1EZ, UK; fax: +44 1223 36033). The respective CCDC numbers are listed in Table 2.

Table 2
Crystal data and details of the refinement for (I), (II), and (V).

	I	II	V
Formula	$C_4H_{11}B\ F_4N_2O_4$	$C_4H_{11}Cl\ N_2O_8$	$C_4H_{11}I\ N_2O_4$
CCDC number	767,861	767,860	767,862
M_r	237.96	250.60	278.05
Crystal size (mm^3)	0.08 × 0.07 × 0.07	0.08 × 0.05 × 0.05	0.50 × 0.20 × 0.15
Crystal system	Triclinic	Triclinic	Monoclinic
Space group	$P\bar{1}$	$P\bar{1}$	$C\,2$
a (Å)	8.6069(2)	8.700(2)	18.589(4)
b (Å)	11.8626(3)	14.842(2)	5.161(1)
c (Å)	14.7597(4)	19.396(2)	20.389(4)
α (°)	104.451(1)	98.748(7)	90
β (°)	106.417(1)	93.056(9)	110.67(3)
γ (°)	94.918(1)	106.053(9)	90
V (Å^3)	1379.85(6)	2366.8(7)	1830.0(6)
Z	6	10	8
D_{calcd} (g cm^{-3})	1.718	1.758	2.018
μ(Mo Kα) (cm^{-1})	0.189	0.435	3.476
F(0 0 0)	732	1300	1072
$h\ k\ l$ range	±12, −17/11, −19/22	−12/10, −21/22, −17/28	±30, ±8, −31/32
T (K)	295(2)	296(2)	293(2)
Reflections measured	16,550	24,812	11,561
Reflections unique	8996	15,531	7612
Data with $F_o > 4\sigma(F_o)$	7438	10,101	6199
R_{int}	0.081	0.0224	0.036
Parameters refined	449	739	288
$R(F)$[a] (for $F_o > 4\sigma(F_o)$)	0.0557	0.0566	0.0322
$wR(F^2)$[a] (all reflections)	0.1703	0.1520	0.0779
Weighting parameters a/b	0.081/0.435	0.065/1.089	0.024/1.484
Flack parameter [22]	–	–	0.13(2)
GoF (F^2)[a]	1.06	1.03	1.02
$\Delta\rho_{fin}$ (max/min) (e Å^{-3})	0.48/−0.47	1.29/−0.51	0.90/−0.95

[a] $R1 = \sum \|F_o| - |F_c\|/\sum|F_o|$, $wR2 = \left[\sum w(F_o^2 - F_c^2)^2/\sum wF_o^4\right]^{1/2}$, $w = 1/\left[\sigma^2(F_o^2) + (a \times P)^2 + b \times P\right], P = (F_o^2 + 2F_c^2)/3$.

In addition to the single crystal analysis, powder diffraction data were collected for compounds I and II. Although single crystal data are superior with regard to determination and refinement of atomic positions and displacement parameters, more accurate lattice parameters were obtained from the powder data by means of the Rietveld method [20]. Powder data were collected at room temperature on a Philips PW3020 X-ray powder diffractometer (Cu Kα radiation (λ = 1.540593 Å) with Bragg–Brentano geometry. The powder patterns were submitted to the Powder Diffraction File [21]. It is noteworthy that although the unit cell parameters of compounds (I) and (II) are quite different, the diffractograms are rather similar (Fig. 1). This fact can be explained by the similarity of the arrangement of building units in the structure (see below).

2.3. Registration of IR and Raman spectra

Fourier-transform Raman spectra were registered by a NXP FT-Raman Module of a Nicolet 5700 spectrometer (number of scans: 512 ($\mathrm{2Gly\cdot HBF_4}$ (I)), 256 ($\mathrm{2Gly\cdot HClO_4}$ (II)), 768 ($\mathrm{Gly\cdot HBF_4}$ (III)), 512 ($\mathrm{Gly\cdot HClO_4}$ (IV), laser power at sample: 0.50 W (I), 0.18 W (II), 0.37 W (III), 0.09 W (IV), resolution 4 $\mathrm{cm^{-1}}$) at room temperature. The same spectrometer was used for measuring attenuated total reflection Fourier-transform infrared spectra (FTIR ATR) (ZnSe prism, 4000–650 $\mathrm{cm^{-1}}$, Happ-Genzel apodization, ATR distortion is corrected, number of scans 32, resolution 4 $\mathrm{cm^{-1}}$). Parts of spectra in the region 650–400 $\mathrm{cm^{-1}}$ were taken from FTIR spectra registered with Nujol mull (4000–400 $\mathrm{cm^{-1}}$, number of scans 32, resolution 2 $\mathrm{cm^{-1}}$).

3. Results and discussion

3.1. Crystal structures

Two of the three crystal structures presented in this work, namely $\mathrm{2Gly\cdot HBF_4}$ (I) and $\mathrm{2Gly\cdot HClO_4}$ (II), are expected to show

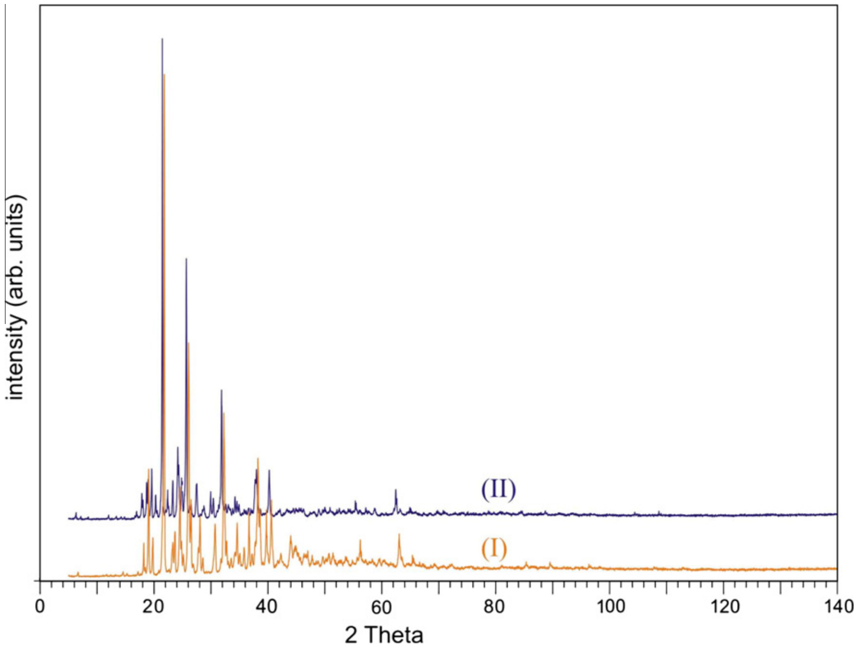

Fig. 1. X-ray Powder diagrams of $\mathrm{GlyH\cdot Gly\cdot BF_4}$ (I) and $\mathrm{GlyH\cdot Gly\cdot ClO_4}$ (II). Note the similarity of the diagrams in spite of the different unit cell parameters. This similarity results from the likewise arrangement of the building units (see text).

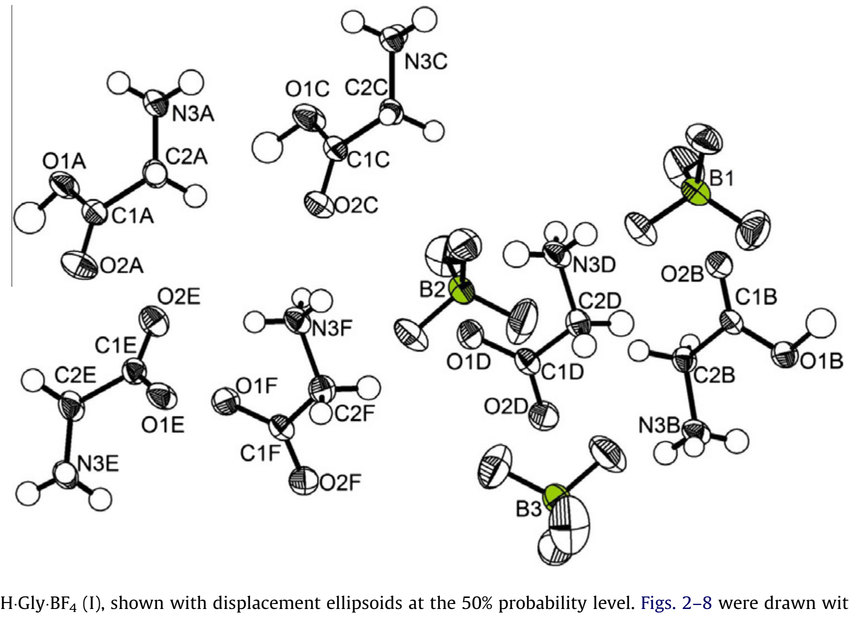

Fig. 2. The connectivity in $\mathrm{GlyH\cdot Gly\cdot BF_4}$ (I), shown with displacement ellipsoids at the 50% probability level. Figs. 2–8 were drawn with the program DIAMOND [23].

Table 3
Hydrogen bonds in (I), (II), and (V) (in Å and °).

	D—H	H···A	D···A	DHA
Compound (I)				
O1A—H1A···O1D	1.06(3)	1.41(3)	2.462(1)	172(3)
O1B—H1B···O1E	1.11(3)	1.36(3)	2.465(1)	179(3)
O1C—H1C···O1F	1.15(3)	1.30(3)	2.453(1)	174(3)
N3C—H31C···F34	0.89	2.11	2.943(2)	155.6
N3C—H32C···F22	0.89	2.01	2.839(1)	155.5
N3C—H33C···O2B	0.89	1.95	2.830(2)	168.9
N3A—H31A···O2F	0.89	2.08	2.963(2)	173.0
N3A—H32A···O2B	0.89	2.34	3.083(2)	141.2
N3A—H33A···O2D	0.89	1.98	2.849(2)	165.2
N3B—H31B···F12	0.89	2.06	2.913(2)	161.0
N3B—H32B···F31	0.89	2.12	2.913(2	147.5
N3B—H33B···O2C	0.89	1.94	2.823(2)	169.1
N3E—H31E···O2F	0.89	1.99	2.854(2)	162.5
N3E—H32E···F32	0.89	2.26	2.980(2)	138.1
N3E—H33E···O2D	0.89	2.03	2.915(2)	173.9
N3D—H31D···O2A	0.89	1.94	2.815(2)	167.5
N3D—H32D···F14	0.89	2.06	2.877(1)	152.7
N3D—H33D···F23	0.89	2.05	2.895(2)	157.9
N3F—H31F···O2E	0.89	1.98	2.844(2)	164.7
N3F—H32F···F21	0.89	2.32	2.999(2)	132.8
N3F—H33F···O2E	0.89	2.04	2.928(2)	173.8
Compound (II)				
O1A—H1A···O1F	0.82	1.68	2.474(2)	163.7
O1B—H1B···O1G	1.02(2)	1.45(2)	2.464(2)	178(4)
O1C—H1C···O1H	0.95(2)	1.58(2)	2.457(2)	153(3)
O1D—H1D···O1I	0.82	1.65	2.464(2)	173.2
O1E—H1E···O1J	0.82	1.65	2.466(2)	172.2
N3A—H31A···O2H	0.89	1.95	2.824(3)	166.5
N3A—H32A···O12	0.89	2.33	3.049(3)	138.2
N3A—H33A···O2H	0.89	2.06	2.948(3)	172.5
N3B—H31B···O2G	0.89	1.95	2.832(2)	170.6
N3B—H32B···O2D	0.89	2.43	3.150(2)	138.0
N3B—H33B···O2J	0.89	2.06	2.937(3)	168.1
N3C—H31C···O2I	0.89	2.08	2.944(3)	164.7
N3C—H33C···O2F	0.89	1.94	2.820(3)	172.7
N3D—H31D···O43	0.89	2.13	2.980(3)	159.8
N3D—H32D···O53	0.89	2.14	2.931(3)	148.4
N3D—H33D···O2E	0.89	1.95	2.822(2)	168.2
N3E—H31E···O2D	0.89	1.94	2.820(2)	168.7
N3E—H32E···O31	0.89	2.11	2.907(3)	148.7
N3E—H33E···O13	0.89	2.10	2.937(3)	156.3
N3F—H31F···O2C	0.89	1.91	2.795(3)	173.1
N3F—H32F···O11	0.89	2.25	3.006(3)	142.9
N3F—H33F···O23	0.89	2.12	2.984(3)	164.4
N3G—H31G···O2B	0.89	1.93	2.811(3)	168.4
N3G—H32G···O41	0.89	2.13	2.934(3)	149.8
N3G—H33G···O33	0.89	2.15	3.006(3)	162.6
N3H—H31H···O52	0.89	2.15	3.005(3)	159.5
N3H—H32H···O21	0.89	2.09	2.913(2)	153.7
N3H—H33H···O2A	0.89	1.92	2.800(3)	169.5
N3I—H31I···O2G	0.89	2.03	2.909(3)	167.2
N3I—H32I···O51	0.89	2.26	2.995(3)	139.4
N3I—H33I···O2J	0.89	1.96	2.845(3)	170.1
N3J—H31J···O2I	0.89	1.96	2.840(3)	171.4
N3J—H32J···O32	0.89	2.25	2.982(3)	138.9
N3J—H33J···O2F	0.89	2.05	2.921(3)	164.9
Compound (V)				
O1C—H1C···O1A	1.00(2)	1.45(2)	2.448(4)	170(6)
O1B—H1B···O1D	0.98(2)	1.55(3)	2.492(4)	159(5)
N3A—H31A···I1	0.91(4)	2.72(4)	3.583(3)	159(3)
N3A—H32A···O1C	0.85(5)	2.29(5)	3.036(4)	146(4)
N3A—H33A···O1D	0.98(4)	1.93(4)	2.899(4)	171(3)
N3B—H31B···I2	0.76(6)	2.81(6)	3.541(3)	164(5)
N3B—H32B···I1	0.93(4)	2.71(4)	3.631(3)	172(4)
N3B—H33B···I2	0.86(5)	2.91(5)	3.633(3)	143(4)
N3C—H31C···I2	1.00(7)	2.60(7)	3.581(4)	170(5)
N3C—H32C···I2	0.80(6)	2.91(6)	3.681(5)	163(5)
N3C—H33C···O2C	0.84(4)	2.02(5)	2.846(4)	168(4)
N3D—H31D···I1	0.79(6)	2.79(6)	3.563(4)	167(5)
N3D—H32D···O2D	0.82(4)	2.02(4)	2.808(4)	164(6)
N3D—H33D···I1	0.91(6)	2.81(6)	3.639(4)	152(4)

similar or even isotypic structures, based on their chemical analogy. However, the crystallographic parameters alone show that there are considerable differences.

3.1.1. *GlyH·Gly·BF$_4$ (I)*

As illustrated in Fig. 2, the crystal structure of (I) consists of pairs of glycine moieties, each with one in its zwitterionic and the other in a cationic state. As in other compounds of amino acids of the type (A···A$^+$·X$^-$), the glycine–glycinium-pairs form dimers via one strong —COOH···$^-$OOC— hydrogen bond (O···O distances range from 2.453(1) to 2.465(1) Å). Furthermore, they are part of a hydrogen bond network connecting all building units to an extensive three-dimensional hydrogen-bonded lattice (Table 3). This includes the BF_4^- anions which charge-counterbalance the glycinium cations. As indicated by the rather large unit cell (V = 1379.85(6) Å^3), there are several crystallographically different glycine, glycinium and BF$_4$ moieties, precisely three in the asymmetric unit (thus Z = 6). The glycine and glycinium molecules are oriented roughly parallel to each other. In fact, there are two preferred orientations: The moieties A, C, and E are aligned more or less parallel (1 5 0), whereas B, D, and F are more or less parallel (1 $\bar{6}$ 0) (Fig. 3). Within the molecules comprising the structure, the bond lengths and angles are in accordance with the values usually given in the literature (Table 4). Both glycine and glycinium groups are slightly twisted out of planarity (absolute values of the O—C—C—N torsion angles range from 162.2(1) to 166.4(1)°).

3.1.2. *GlyH·Gly·ClO$_4$ (II)*

When comparing the crystallographic data of (I) with that of (II), the first striking difference is the even larger unit cell of (II) (V = 2366.8(7) Å^3, Fig. 4). It comprises ten glycine, glycinium and ClO_4^- anions each (thus Z = 10), five of each in the asymmetric unit. As in (I), the orientation of all amino acid moieties is similar – all are oriented roughly parallel to (0 0 1), again in two preferred orientations. These are more or less (1 0 5) for moieties A, C, D, J, and G and (1 0 $\bar{7}$) for B, E, F, H, and I (Fig. 5). Another similarity to (I) is the fact that there are glycine–glycinium-pairs, connected via

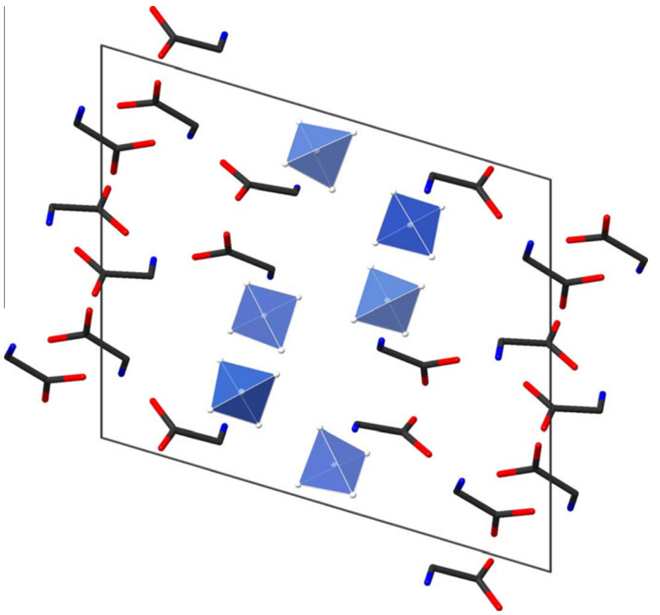

Fig. 3. Packing diagram of GlyH·Gly·BF$_4$ (I) viewed along [1 0 0]. BF$_4$-groups displayed as tetrahedra, hydrogen atoms are omitted for clarity.

Table 4
Geometric parameters for (I), (II), and (V) (in Å and °). The torsion angles are calculated via the *trans*-oxygen atom and are given as absolute values.

Compound (I)	A	B	C	D	E	F
O1—C1	1.294(2)	1.294(2)	1.286(2)	1.265(2)	1.273(2)	1.270(2)
O2—C1	1.220(2)	1.224(2)	1.231(2)	1.241(2)	1.235(2)	1.235(2)
N3—C2	1.485(2)	1.473(2)	1.474(2)	1.468(2)	1.486(2)	1.480(2)
C1—C2	1.514(2)	1.516(2)	1.510(2)	1.519(2)	1.516(2)	1.515(2)
O2—C1—O1	125.2(1)	125.0(1)	124.9(1)	125.8 (1)	125.6(1)	125.8(1)
O2—C1—C2	120.6(1)	120.7(1)	120.1(1)	118.9 (1)	118.9(1)	118.9(1)
O1—C1—C2	114.2(1)	114.4(1)	115.0(1)	115.3(1)	115.4(1)	115.3(1)
N3—C2—C1	112.3(1)	112.1(1)	111.8(1)	111.2(1)	112.2(1)	112.2(1)
O*—C1—C2—N3	164.5(1)	162.2(1)	164.2(1)	165.67(1)	162.47(1)	166.4(1)

BF_4-groups	Anion 1	Anion 2	Anion 3
B—F1	1.380(2)	1.370(2)	1.368(2)
B—F2	1.382(2)	1.381(2)	1.370(2)
B—F3	1.394(2)	1.392(2)	1.380(2)
B—F4	1.395(2)	1.399(2)	1.396(2)
Mean	1.388	1.386	1.379

Compound (II)	A	B	C	D	E	F	G	H	I	J
O1—C1	1.299(3)	1.291(3)	1.286(3)	1.282(2)	1.277(2)	1.260(3)	1.257(3)	1.253(3)	1.268(3)	1.270(3)
O2—C1	1.212(3)	1.219(3)	1.220(3)	1.225(3)	1.228(2)	1.245(2)	1.237(3)	1.244(3)	1.235(3)	1.235(3)
N3—C2	1.511(3)	1.510(3)	1.514(3)	1.513(3)	1.514(3)	1.516(3)	1.514(3)	1.515(3)	1.515(3)	1.516(3)
C1—C2	1.484(3)	1.483(3)	1.482(3)	1.479(3)	1.478(3)	1.465(3)	1.473(3)	1.467(3)	1.483(3)	1.482(3)
O2—C1—O1	125.0(2)	125.1(2)	125.7(2)	124.8(2)	124.7(2)	125.2(2)	125.8(2)	125.6(2)	125.7(2)	126.1(2)
O2—C1—C2	121.0(2)	120.2(2)	119.9(2)	120.2(2)	120.1(2)	118.9(2)	118.7(2)	118.8(2)	118.7(2)	118.4(2)
O1—C1—C2	114.0(2)	114.6(2)	114.4(2)	114.9(2)	115.1(2)	115.9(2)	115.5(2)	115.6(2)	115.6(2)	115.5(2)
N3—C2—C1	112.7(2)	112.7(2)	112.7(2)	112.0(2)	112.0(2)	111.4(2)	111.4(2)	111.2(2)	112.3(2)	112.3(2)
O*—C1—C2—N3	162.4(2)	165.1(2)	165.1(2)	163.0(2)	162.5(2)	162.8(2)	165.4(2)	165.6(2)	164.0(2)	164.7(2)

ClO_4-groups	Anion 1	Anion 2	Anion 3	Anion 4	Anion 5
Cl—O1	1.421(2)	1.425(2)	1.424(2)	1.427(2)	1.421(2)
Cl—O2	1.428(2)	1.436(2)	1.425(2)	1.432(2)	1.425(2)
Cl—O3	1.431(2)	1.441(2)	1.428(2)	1.440(2)	1.425(2)
Cl—O4	1.443(2)	1.442(2)	1.440(2)	1.441(2)	1.441(2)
Mean	1.431	1.436	1.429	1.435	1.428

Compound (V)	A	B	C	D
O1—C1	1.278(4)	1.300(4)	1.287(3)	1.272(4)
O2—C1	1.219(4)	1.221(4)	1.235(4)	1.226(4)
C1—C2	1.520(5)	1.499(4)	1.500(6)	1.508(6)
C2—N3	1.473(4)	1.470(4)	1.476(4)	1.480(4)
O2—C1—O1	126.4(3)	125.1(3)	125.7(3)	126.6(3)
O2—C1—C2	119.3(3)	123.6(3)	120.3(3)	119.1(3)
O1—C1—C2	114.3(3)	111.3(3)	114.0(3)	114.3(3)
N3—C2—C1	111.4(2)	111.1(3)	110.9(4)	110.8(3)
O*—C1—C2—N3	168.4(3)	178.7(3)	175.7(3)	173.4(3)

strong H-bonds (O···O distances range from 2.457(2) to 2.474(2) Å), as well as an extensive hydrogen bond network incorporating the ClO_4^- anions to form a three-dimensional framework. Finally, the geometry of the molecules is also within range of the ordinary values (Table 4).

Since practically all these features correspond to those of (I), the different unit cell sizes are puzzling. Only when examining the topology of the building units in both compounds, the issue becomes clear: The anionic tetrahedra in both compounds are arranged in rows (parallel to [0 1 0] in (I) and to [0 0 1] in (II)). These rows are not straight but zig-zagged, with steps of pairs of tetrahedra. The offsets differ in both structures, the tetrahedral rows alternate according to the following patterns: In the case of (I), the offset is one step to the right, then two to the left (when viewed along [1 0 0]), in (II) it is two to the left, three to the right (Fig. 6). Therefore, the difference of the unit cell parameters is obvious: The distances between two adjacent rows is comparable, both within the layer of the zig-zag row (c = 14.7597(4) Å in (I) and b = 14.842(2) Å in (II)) and between these layers (a = 8.6069(2) and 8.700(2) Å in (I) and (II), respectively). The period length of

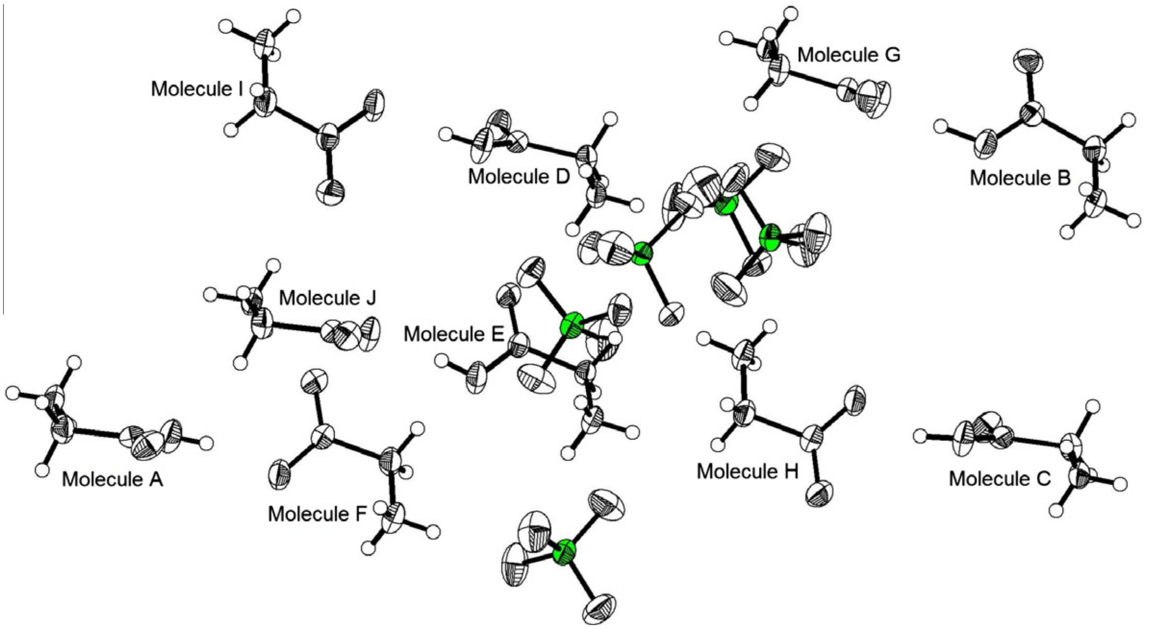

Fig. 4. The connectivity in GlyH·Gly·ClO_4 (II), shown with displacement ellipsoids at the 50% probability level. For clarity, only the molecules are labeled, the labeling of the individual atoms within the molecules is as in Fig. 2.

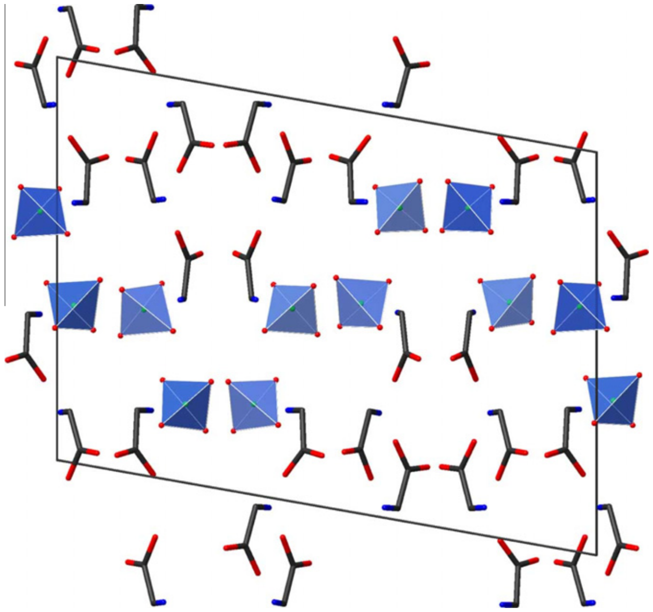

Fig. 5. Packing diagram of GlyH·Gly·ClO_4 (II) viewed along [1 0 0]. ClO_4 groups displayed as tetrahedra, hydrogen atoms are omitted for clarity.

the rows, *b* in (I) and *c* in (II), viz. 11.8626(3) and 19.396(2) Å, respectively, relate to each other as 3:5. The same relation, consequently, exists between the unit cell volumes and values of *Z*.

3.1.3. GlyH·Gly·I (V)

Apparently, the structure of (V) is clearly different since the charge-counterbalance for the glycinium cations are single-atom anions, namely iodide ions, instead of tetrahedral groups (Fig. 7). Nevertheless, there are similarities to the structures of the above species. This certainly applies to the geometries of the glycinium and glycine moieties, which again correspond well to the expected values (Table 4), as well as the strong hydrogen bonds that connect glycinium–glycine dimers (Table 3). There is also some regularity in the arrangement of the molecules (Fig. 8), which are either parallel to (0 1 6) and (0 1 $\bar{6}$) in the case of molecules A and C or to (4 1 0) and ($\bar{4}$ 1 0) for molecules B and D. Most remarkably, however, the anions are also arranged in distinct rows (along [0 0 1]) of zig-zag pairs. In contrast to the above structures, the offset is one to the left and one to the right when viewed along [1 0 0]. When comparing this redetermined structure with the original one [4], a few differences become apparent. Of course, since the previous analysis was performed in 1972 with a scintillation detector diffractometer, methods were cruder and the data therefore less thorough. Thus, no hydrogen positions were refined in [4],

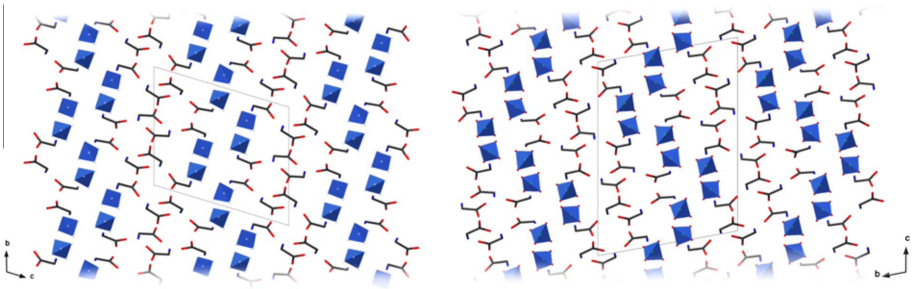

Fig. 6. Comparison of the packing modes in GlyH·Gly·BF_4 (I) (left), and GlyH·Gly·ClO_4 (II) (right), both viewed along [1 0 0]. The zig-zag rows of pairs of tetrahedra are oriented vertically. Note the different offsets in (I) and (II): one step left, two right for (I) and three steps left, two right for (II), thus the period lengths relate to each other as 3:5.

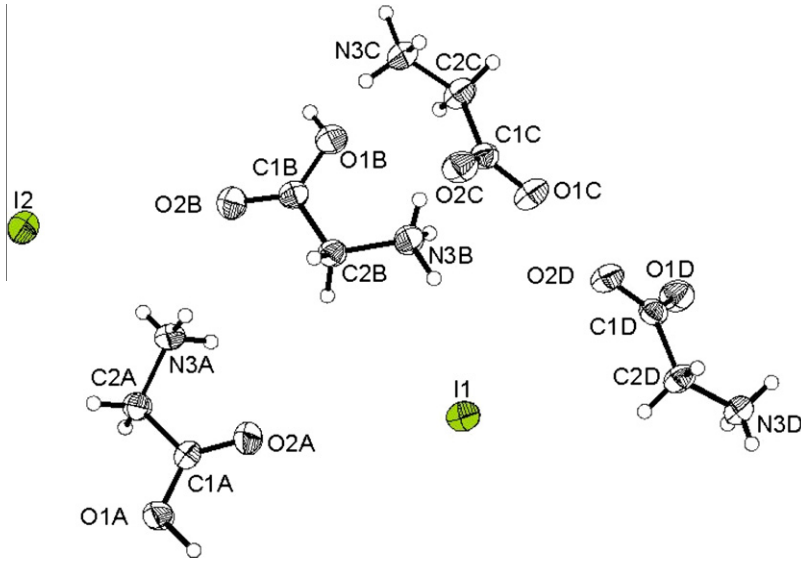

Fig. 7. The connectivity in GlyH·Gly·I (V), shown with displacement ellipsoids at the 50% probability level. Labeling of the atoms in the glycine molecules as in (I).

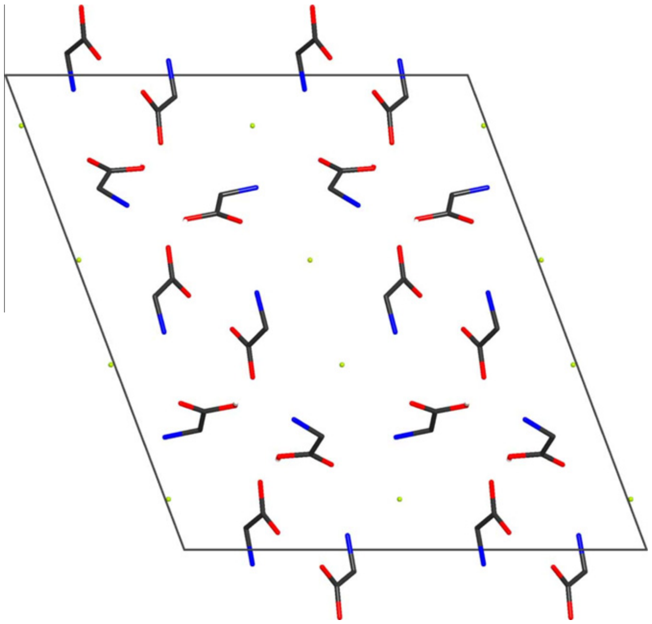

Fig. 8. Packing diagram of GlyH·Gly·I (V) viewed along [0 1 0]. Hydrogen atoms are omitted for clarity.

and consequently, the hydrogen bonds calculated from the D···A-distances only. For comparison purposes, we labeled the glycine moieties in the same order as in [4], although keeping our labeling scheme as used in (I) and (II). Therefore, the moieties Gly(1), Gly(3), Gly(2), Gly(4) in [4] correspond to Gly(A), Gly(B), Gly(C), Gly(D) in this paper, respectively. For the iodine ions the labels I1 and I2 were kept. The O···O distances in the dimers Gly(A)···Gly(C) (2.448(4) Å) and Gly(B)···Gly(D) (2.492(4) Å) correspond satisfactorily to 2.436 Å in Gly(1)···Gly(2) and 2.477 Å in Gly(3)···Gly(4), respectively. Also, the bond lengths in Gly(D) and Gly(4) agree well. However, the agreement of the bond lengths in Gly(A), Gly(B), Gly(C) and Gly(1), Gly(3), Gly(2) is not so good, e.g. in Gly(A) we find 1.278(4) Å and 1.219(4) Å for C1A—O1A and C1A—O2A, respectively, whereas in Gly(1) the respective values are 1.309(15) Å (C5—O6) and 1.166 Å (C5—O7) [4]. Otherwise, our data match the older and thus confirm the structure established by Piret et al. [4]. In this work, however, all hydrogen positions could be located and refined without constraints, and although the N—H-distances show considerable variation, nevertheless we could identify distinct hydrogen bonds (Table 3), some of which differ from those given in [4].

3.2. Vibrational spectra

The vibrational spectra of 2Gly·HBF$_4$ (I) and 2Gly·HClO$_4$ (II) are shown in Figs. 9 and 10. For comparison purposes, the spectra of Gly·HBF$_4$ (III) and Gly·HClO$_4$ (IV) are shown as well in Figs. 11 and 12. Wavenumbers of the peaks and assignment of some characteristic vibrations are collected in Table 5. Assignment of the peaks was made taking into account the results of spectroscopic investigation of GlyH·Gly·NO$_3$ [24], Ref. [25], and tetrafluoroborates and perchlorates of L-arginine [26] and L-histidine [27].

As was mentioned in Section 3.1, both compounds (I) and (II) crystallize in centrosymmetrical triclinic structure and contain dimeric cations (GlyH···Gly) and respective BF$_4^-$ and ClO$_4^-$ anions. As said above, the distinction is the number of independent formula units – three in (I) and five in (II). Of course, their vibrational spectra have substantial similarity due to presence of similar (GlyH···Gly) dimeric cations. The mean value of O···O distance of the COOH···$^-$OOC hydrogen bond in the (GlyH···Gly) dimers is 2.46 Å. As shown previously by Ichikawa [28], such a strong hydrogen bond leads to a noticeable decrease of the C—OH bond distance and a respective increase of the C=O bond length in the COOH group. In our case, the mean values are 1.29 and 1.22 Å for the C—OH and C=O bond lengths, respectively. These values are in good agreement with the correlation shown in [28]. Simultaneously, the bond lengths in the COO$^-$ group also shift due to a strong hydrogen bond. The C—O contact that forms the hydrogen bond becomes longer, while the other one becomes shorter. In (I), these values are 1.27 Å and 1.24 Å, respectively, while in case of (II) they are 1.26 Å and 1.24 Å compared to the normal mean value (1.25 Å) in a perfectly symmetric, mesomeric COO$^-$ group without a strong hydrogen bond. Such strong hydrogen bonds in the (GlyH···Gly) dimers may result in some alteration of the vibrational spectra.

The GlyH cation is characterized by the presence of an absorption band higher than 1700 cm^{-1} caused by stretching vibration of the C=O bond (see e.g. GlyH·Cl [25] with the absorption band at

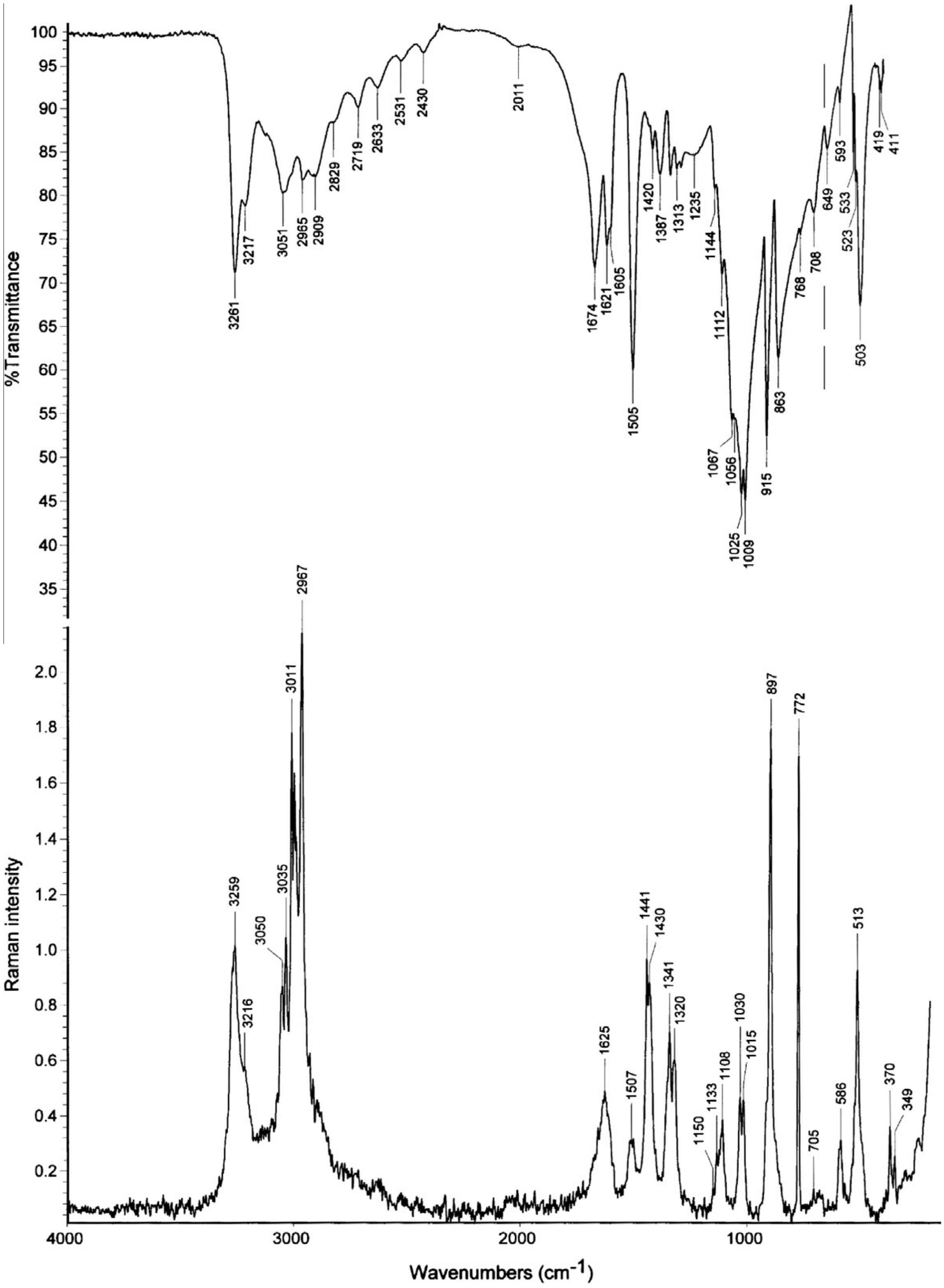

Fig. 9. Powder IR and Raman spectra of GlyH·Gly·BF_4 (I).

1745 cm^{-1}). In the spectra of (III) and (IV), these expected bands are observed, namely at 1728 cm^{-1}, 1709 cm^{-1} (IR), and 1750 cm^{-1} (R) in the spectrum of (III) (Fig. 11) and at 1726 cm^{-1}, 1707 cm^{-1} (IR), and 1738 cm^{-1}, 1711 cm^{-1} (R) in the spectrum of (IV) (Fig. 12). A dimeric (GlyH···Gly) cation also can produce a band higher than 1700 cm^{-1}, due to the presence of GlyH, but depending on strength, symmetry and nature of the hydrogen bond, the wavenumber of this vibration may be shifted to the intermediate region between typical values of stretching vibration of C=O bond and asymmetric stretching vibration of the COO^- group. In the IR spectra of (I) and (II) (Figs. 9 and 10) this mode is assigned to the bands clearly visible at 1674 cm^{-1} and 1667 cm^{-1}, respectively. The

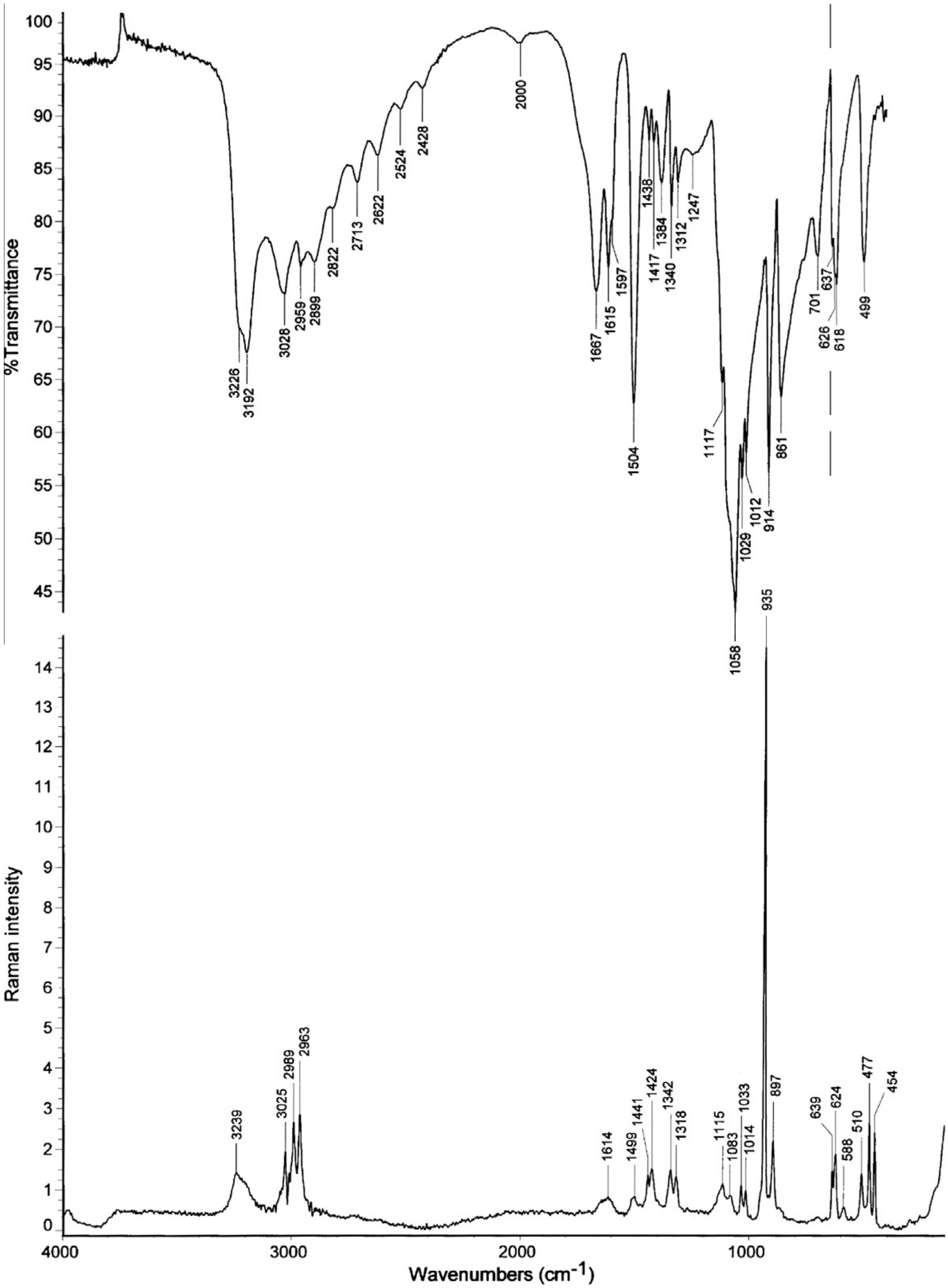

Fig. 10. Powder IR and Raman spectra of GlyH·Gly·ClO_4 (II).

corresponding bands in the Raman spectra are not easily visible due to their very low intensity.

The tetrahedral BF_4^- and ClO_4^- anions are characterized by two stretching (ν_{as} and ν_s) and two deformation (δ_{as} and δ_s) vibrations. For free anions, all these are active in the Raman spectra, while in the IR spectra ν_s and δ_s are inactive [29]. The Raman line corresponding to ν_s for ClO_4^- is very intensive and characteristic by its frequency. One can find it easily in Figs. 10 and 12 at 935 cm^{-1} and 936 cm^{-1}, respectively. The respective ν_s line for BF_4^- anion is not so intensive, but also characteristic by its frequency. This vibration is observed at 772 cm^{-1} in Figs. 9 and 11. The asymmetric stretching vibration (ν_{as}) for both anions also is very characteristic in the IR spectra. The very strong band at 1005 cm^{-1} (Fig. 11) as well as the band with peaks at 1067, 1056, 1025 and 1009 cm^{-1}

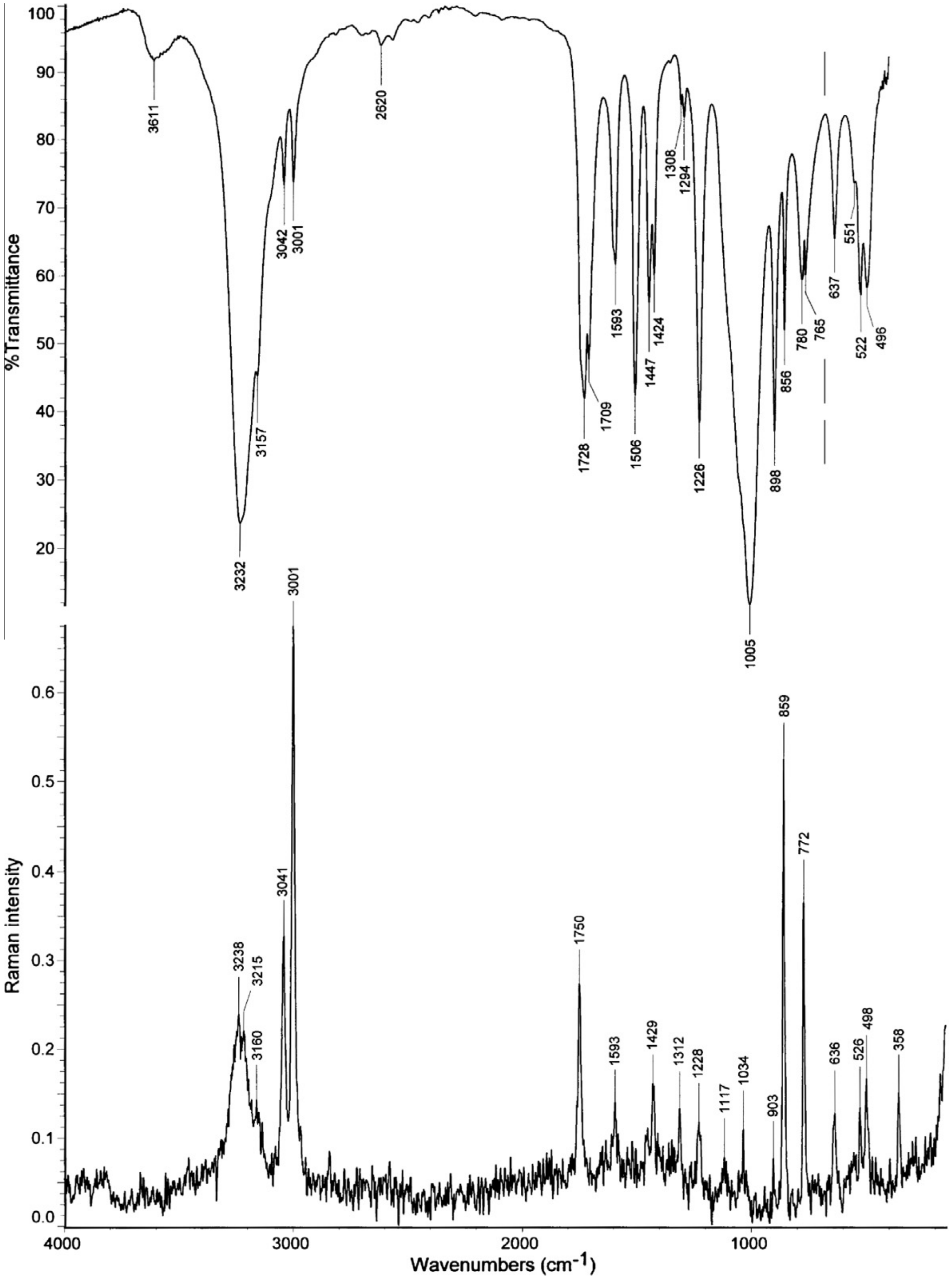

Fig. 11. Powder IR and Raman spectra of GlyH·BF_4 (III).

have been assigned to ν_{as} of the BF_4^- anion. The respective vibration of ClO_4^- is visible as a band at 1058 cm^{-1} (Fig. 10) and a band with peaks at 1055 cm^{-1} and 1033 cm^{-1} (Fig. 12). The assessments of stretching vibrations of N—H and C—H bonds in the high-frequency region as well as some other vibrations of (I) and (II) are made in Table 5. In addition, absorption bands at 3599 cm^{-1} and 3611 cm^{-1} (Figs. 11 and 12) can be found, which indicate the presence of absorbed water due to the high hygroscopicity of the compounds (in spite of keeping them in a closed vessel with silica gel). It is difficult to point out the important and interesting stretching vibrations of O—H-bonds in dimeric cations in Figs. 9 and 10 because there are strong absorption bands due to asymmetric stretching vibrations of BF_4^- and ClO_4^- anions in the region near 1000 cm^{-1} expected for ν(O—H).

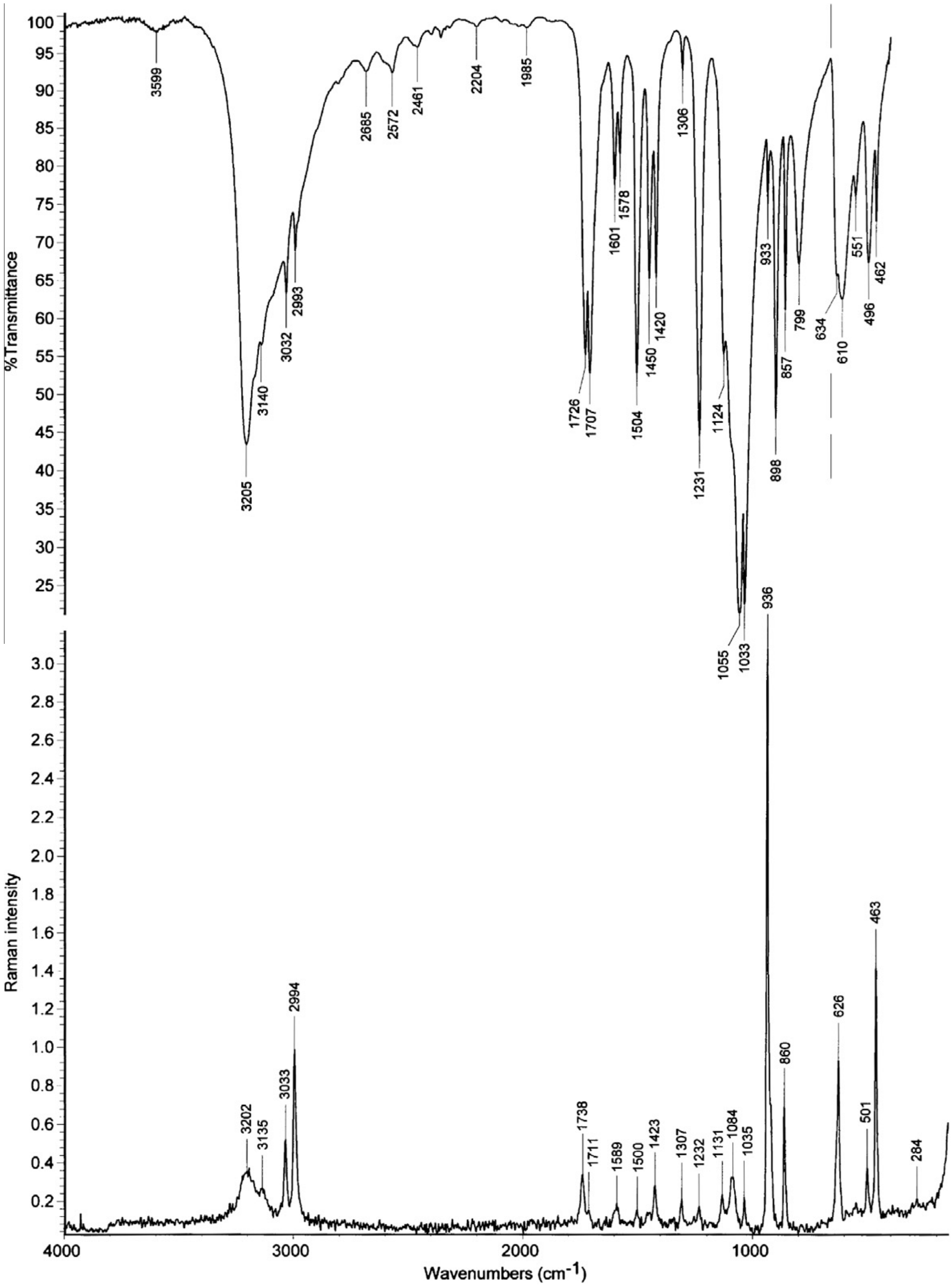

Fig. 12. Powder IR and Raman spectra of GlyH·ClO$_4$ (IV).

4. Conclusion

Within the large family of compounds of amino acids and inorganic anions, we have synthesized and characterized new members with glycinium as the amino acid cation. These are the tetrafluoroborates (GlyH·Gly·BF$_4$) (I) and (GlyH·BF$_4$) (III), the perchlorates (GlyH·Gly·ClO$_4$) (II) and (GlyH·ClO$_4$) (IV), as well as the previously known iodide (GlyH·Gly·HI) (V). For the (GlyH···Gly) members, the crystal structures were determined, and the typical (A···A$^+$·X$^-$) arrangement was found, i.e. the glycine–glycinium-pairs forming dimers via one strong COOH···$^-$OOC hydrogen bond. Since glycine is the only non-chiral amino acid, centrosymmetrical structures are possible, as it is realized in the structures of (I) and (II) in the triclinic space groups $P\bar{1}$, with remarkably large unit cells ($Z = 6$ and 10, respectively). The structure of (V) was redetermined and found to be non-centrosymmetrical (space group $C2$), a feature

Table 5
Wavenumbers and assignments in the IR and Raman spectra of GlyH·Gly·BF_4 (I) and GlyH·Gly·ClO_4 (II), GlyH·BF_4 (III), GlyH·ClO_4 (IV).

(I)		(III)		(II)		(IV)		Assignment
IR	Raman	IR	Raman	IR	Raman	IR	Raman	
3261	3259	3232	3238; 3215	3226 sh	3239	3205	3202	ν_{as}(NH) NH_3^+
3217	3216 sh			3192				ν_{as}(NH) NH_3^+
3051	3050	3157	3160			3140	3135	ν_s(NH) NH_3^+
	3035			3028	3025			ν_s(NH) NH_3^+
	3011; 2999	3042	3041			3032	3033	ν(CH) CH_2
	2991	3001	3001		2989	2993	2994	ν(CH) CH_2
2965	2967			2959	2963			ν(CH) CH_2
2909				2899				ν(CH) CH_2
2829				2822		2807		Sum tone
2719		2698		2713				Sum tone
2633		2620		2622		2685		Sum tone
2531		2569		2524		2572		Sum tone
2430				2428		2461		Sum tone
						2399		
						2204		
2011				2000		1985		Sum tone
1674		1728; 1709	1750	1667		1726; 1707	1738; 1711	ν(C=O)
1621	1625			1615	1614			$\nu_{as}(COO^-)$
1605 sh		1593	1593	1595 sh		1601; 1578	1589	$\delta_{as}(NH_3^+)$
1505	1507	1506		1504	1499	1504	1500	$\delta_s(NH_3^+)$
1434	1441	1447		1438	1441; 1424	1450	1457	$\delta(CH_2)$
1420	1430	1424	1429	1417		1420	1423	$\delta(CH_2)$
1387				1384				$\nu_s(COO^-$
1341; 1313; 1294	1341; 1320	1308; 1294	1312	1340; 1312	1342; 1318	1306	1307	$\omega(CH_2)$
1235		1226	1228	1247		1231	1232	ν(C—OH)
1144	1133					1124	1131	$\rho(NH_3^+)$
1112	1108		1117	1117 sh	1115			$\rho(NH_3^+)$
1067; 1056								$\nu_{as}(BF_4^-)$
				1086sh		1090sh		$\nu_{as}(ClO_4^-)$
				1067sh	1083	1055vs	1084; 1035	
				1058 vs		1033vs		
1025; 1009	1030; 1015	1005	1034					ν(C—N); $\nu_{as}(BF_4^-)$
				1029; 1012	1033; 1014			ν(C—N)
					935 vs	933	936vs	$\nu_s(ClO_4)$
							921sh	
915	897	898	903	914	897	898		$\rho(CH_2)$
863		856	859	861		857	860	ν(C—C)
		780				799		
	772 vs		772					$\nu_s(BF_4^-)$
768		765						
708				701				$\delta(COO^-)$
649		637	636					
				637; 626	639; 624	634	626	$\delta_{as}(ClO_4^-)$
				618		610		
593	586				588			$\omega(COO^-)$
		551				551		
533; 523	513	522	526					$\delta_{as}(BF_4^-)$
503		496	498	499	510	496	501	δ(CCO)
					477; 454	462	463	$\delta_s(ClO_4^-)$
419; 411								
	370; 349		358					$\delta_s(BF_4^-)$
							284	

quite common for compounds of glycine and inorganic materials [30]. As has been shown before, this simplest of amino acids is a potent species for the formation of new and interesting materials [31].

Acknowledgments

The present research has been carried out in frame of Project #0111 supported by the Government of Armenia and ANSEF (PS1839 Project).

References

[1] W.S. Frost, J. Am. Chem. Soc. 64 (1942) 1286.
[2] M.J. Buerger, E. Barney, Th. Hahn, Z. Kristallogr. 108 (1956) 130 (see also: Th. Hahn, Z. Kristallogr. 111 (1959) 161).
[3] Th. Hahn, M.J. Buerger, Z. Kristallogr. 108 (1957) 419 (see also: T. Hahn, Z. Kristallogr. 113 (1960) 403).
[4] P. Piret, J. Meunier-Piret, J. Verbist, M. Van Meerssche, Bull. Soc. Chim. Belges 81 (1972) 539.
[5] R. Pepinsky, K. Vedam, S. Hoshino, Y. Okaya, Phys. Rev. 111 (1958) 430.
[6] T. Kai, M. Goto, K. Furuhata, H. Takayanagi, Anal. Sci. 10 (1994) 359.
[7] I. Němec, I. Cisarová, Z. Mička, J. Solid State Chem. 140 (1998) 71.
[8] V.H. Rodrigues, M.M.R.R. Costa, T. Dekola, E. de Matos Gomes, Acta Cryst. E65 (2009) m19.
[9] T. Dekola, D. Isakov, E. de Matos Gomes, V.H. Nunes Rodrigues, M.M.R. Costa, Eur. Phys. J. B 68 (2009) 519.
[10] S. Natarajan, A. Kalyanasundar, J. Suresh, S.A. Martin Britto Dhas, P.L. Nilantha Lakshman, Acta Cryst. E65 (2009) o462.
[11] S. Natarajan, C. Muthukrishnan, S.A. Bahadur, R.K. Rajaram, S.S. Rajan, Z. Kristallogr. 198 (1992) 265.
[12] J.W. Faamau, E.R.T. Tiekink, Z. Kristallogr. 204 (1993) 277.
[13] S. Natarajan, E. Zangrando, Proc. Indian Acad. Sci. Chem. Sci. 104 (1992) 483.
[14] K. Łukaszewicz, A. Pietraszko, J. Stępień-Damm, Pol. J. Chem. 70 (1996) 1441.
[15] K. Łukaszewicz, A. Pietraszko, J. Stępień-Damm, Pol. J. Chem. 70 (1996) 1550.
[16] Nonius, Collect, Nonius BV, Delft (The Netherlands), 2003.

[17] Bruker–Nonius, Apex-II and Saint-Plus (Version 7.06a), Bruker AXS Inc., Madison, Wisconsin, USA, 2004.
[18] Z. Otwinowski, W. Minor, Methods Enzymol., Part A 276 (1997) 307.
[19] G.M. Sheldrick, Acta Crystallogr. A64 (2008) 112.
[20] R.X. Fischer, C.L. Lengauer, E. Tillmanns, R.J. Ensik, C.A. Reiss, E.J. Fantner, Mater. Sci. Forum 133–136 (1993) 287.
[21] PC-PDF, Powder Diffraction File: International Centre for Diffraction Data (ICDD), Newton Square, PA 19073, USA, 1999.
[22] H.D. Flack, Acta Crystallogr. A39 (1983) 876.
[23] G. Bergerhoff, M. Berndt, K. Brandenburg, J. Res. NIST 101 (1997) 221.
[24] J. Baran, A.J. Barnes, H. Ratajczak, Spectrochim. Acta 51A (1995) 197.
[25] M.T. Rosado, M. Leonor, T.S. Duarte, R. Fausto, Vib. Spectrosc. 16 (1998) 35.
[26] A.M. Petrosyan, Vib. Spectrosc. 41 (2006) 97.
[27] A.M. Petrosyan, Vib. Spectrosc. 43 (2007) 284.
[28] M. Ichikawa, J. Cryst. Mol. Struct. 9 (1979) 87.
[29] Kazuo Nakamoto, Infrared and Raman Spectra of Inorganic and Coordination Compounds, Part A, sixth ed., John Wiley and Sons, Inc., 2009.
[30] M. Fleck, Z. Kristallogr. 223 (2008) 222.
[31] A.A. Kaminskii, L. Bohatý, P. Becker, P. Held, H.J. Eichler, H. Rhee, J. Hanuza, Laser Phys. Lett. 6 (2009) 872.